materials proceedings

MDPI

Proceeding Paper

Direct Contacting of 2D Nanosheets by Metallic Nanoprobes †

Filippo Giubileo [1,*], Francesca Urban [1,2], Alessandro Grillo [1,2], Aniello Pelella [1,2], Enver Faella [2] and Antonio Di Bartolomeo [1,2]

[1] CNR-SPIN Salerno Via Giovanni Paolo II 132, 84084 Fisciano, Salerno, Italy; furban@unisa.it (F.U.); agrillo@unisa.it (A.G.); apelella@unisa.it (A.P.); adibartolomeo@unisa.it (A.D.B.)
[2] Physics Department "E. R. Caianiello", University of Salerno, Via Giovanni Paolo II 132, 84084 Fisciano, Salerno, Italy; efaella@unisa.it
* Correspondence: filippo.giubileo@spin.cnr.it
† Presented at the 2nd International Online-Conference on Nanomaterials, 15–30 November 2020; Available online: https://iocn2020.sciforum.net/.

Abstract: We present a simple and fast methodology to realize metal contacts on two-dimensional nanosheets. In particular, we perform a complete characterization of the transport properties of MoS_2 monolayer flakes on SiO_2/Si substrates by using nano-manipulated metallic tips as metallic electrodes directly approached on the flake surface. We report detailed experimental investigation of transport properties and contact resistance in back-gated field effect transistor in which the Si substrate is used as the gate electrode. Moreover, profiting of the n-type conduction, as well as the high aspect ratio at the edge of the MoS_2 flakes, we also explored the possibility of exploiting the material as a field emitter. Indeed, by retracting one of the metallic probes (the anode) from the sample surface, it has been possible to switch on a field-emitted current by applying a relatively low external electric field of few-tens of Volts for a cathode-anode separation distance below 1 μm. Experimental data are then analyzed in the framework of Fowler-Nordheim theory and its extension to the two-dimensional limit.

Keywords: two-dimensional materials; transition metal dichalcogenides; molybdenum disulfide; field-effect transistor; transport properties; field emission

Citation: Giubileo, F.; Urban, F.; Grillo, A.; Pelella, A.; Faella, E.; Di Bartolomeo, A. Direct Contacting of 2D Nanosheets by Metallic Nanoprobes. *Mater. Proc.* **2021**, *4*, 16. https://doi.org/10.3390/IOCN2020-07931

Academic Editors: Ana María Díez-Pascual and Guanying Chen

Published: 11 November 2020

1. Introduction

Molybdenum disulfide (MoS_2) is one of the most investigated transition-metal dichalcogenides (TMDs) for exploitation in next-generation two-dimensional (2D) devices, including field-effect transistors [1–4], solar cells [5], photodetectors [6,7], field emission devices [8–11], chemical or biological sensors [12,13], etc.

MoS_2 has a crystal structure characterized by a hexagonal layer of Mo atoms between two layers of S atoms. Layers are bonded together by van der Waals forces. MoS_2 flakes can be fabricated either by mechanical exfoliation or chemical vapor deposition [14]. Bulk MoS_2 has 1.2 eV indirect bandgap, while mono-layer (1 L) and bilayer (2 L) MoS_2 have 1.8 eV and 1.6 eV indirect bandgap, respectively [15]. Consequently, both 1 L and 2 L MoS_2 can be used to realize field-effect transistors with high On/Off ratio and photoresponse [16]. On the other hand, carrier mobility is typically limited to few-tens $cm^2\ V^{-1}\ s^{-1}$. Moreover, ohmic contacts (with low resistance) are crucial to improving device performance [17].

In this paper, we demonstrate a simple method of realizing electrical contacts on MoS_2 flakes by using nanomanipulated metallic probes inside a scanning electron microscope (SEM). We show that this technique allows complete characterization of the back-gated field-effect transistor (FET), as well as checking the field emission properties of the MoS_2 flake.

2. Materials and Methods

The MoS_2 flakes studied in this work have been grown on Si/SiO_2 substrates by means of a chemical vapour deposition technique, in which S powder and a saturated ammonium heptamolybdate solution have been used as precursors. Few-layer MoS_2 flakes have been characterized by micro-Raman spectroscopy (λ = 532 nm). The experimental setup for electrical characterization is realized inside a SEM chamber (see Figure 1a) provided with two piezo-driven nano-manipulators for precise positioning (step resolution ~5 nm) of metallic probes (tungsten tips). A semiconductor parameter analyzer (Keithley 4200-SCS) is then used as a source-measurement unit, to apply bias up to ±100 V and to measure current with resolution better than 0.1 pA. Electrical measurements are performed at room temperature and in high vacuum (10^{-6} mbar) after gently approaching the tungsten tips on the MoS_2 flake (a real image taken inside the SEM chamber is shown in Figure 1b) and using the Si substrate as a back gate.

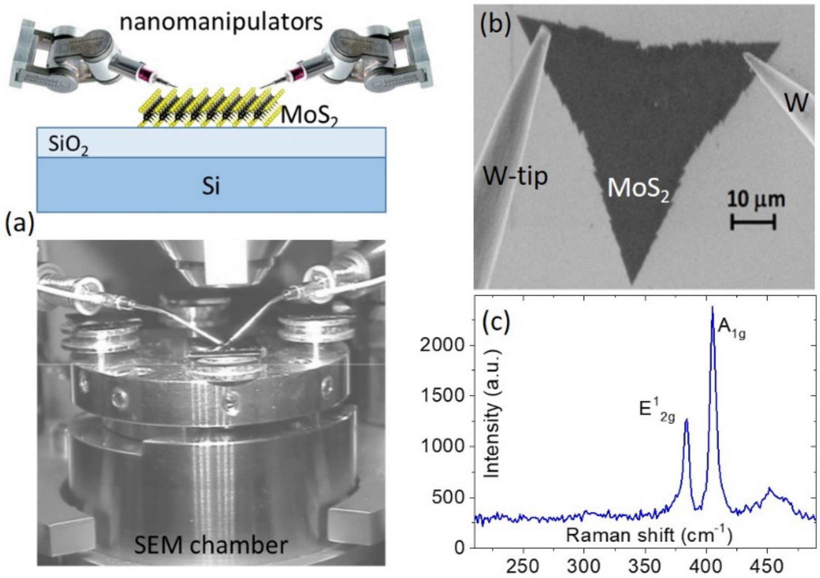

Figure 1. (**a**) Schematic and real image of the nanomanipulators contacting the MoS_2 flake inside the SEM chamber. (**b**) SEM image of a contacted MoS_2 flake. (**c**) Raman spectrum of MoS_2 flake.

Micro-Raman analysis of the MoS_2 flake has shown a spectrum (see Figure 1c) with two peaks corresponding to the E_{2g}^1 and A_{1g} modes, separated by about $20\ \text{cm}^{-1}$, indicating that the sample under investigation is a monolayer.

3. Results and Discussion

In Figure 2a, we report the output characteristics ($I_{ds} - V_{ds}$) measured in the range of ±0.5 V for different values of the gate voltage (V_{gs}). We notice a slight rectification that can be explained as the result of asymmetric Schottky barriers forming at the tungsten/MoS_2 interfaces [3]. By varying the distance between the two tungsten tips, we can modulate the channel length of the FET, thus realizing an experiment based on the Transfer Length Method (TLM) [18,19] to evaluate the contact resistance at the tungsten/MoS_2 interface. In Figure 2b, we show the measured total resistance R_{tot} versus d, with $R_{tot} = 2R_c + \frac{R_s}{W}d$, where R_c is the contact resistance, R_s is the MoS2 sheet resistance, W is the channel width (assumed to be equal to the tip diameter, 200 nm), and d is the channel length, i.e., the separation between the two tips. Experimental data have linear behavior, from which specific area contact resistivity and sheet resistance can be evaluated as $\rho_c \approx 4 \times 10^{-2}\ \Omega\text{cm}^2$ and $R_s \approx 10^8\ \Omega/\square$ from the intercept and the slope of the linear fit, respectively.

The transfer characteristics ($I_{ds} - V_{gs}$) reported in Figure 2c have been measured for different gate voltage ranges up to ±60 V, with $V_{ds} = -5$ V, and by positioning the tungsten tips at separation of 13 μm. The device has n-type behavior, with a threshold voltage of about -10 V, and it can be explained in terms of chemisorption of oxygen on MoS_2 or sulphur vacancies [20–22].

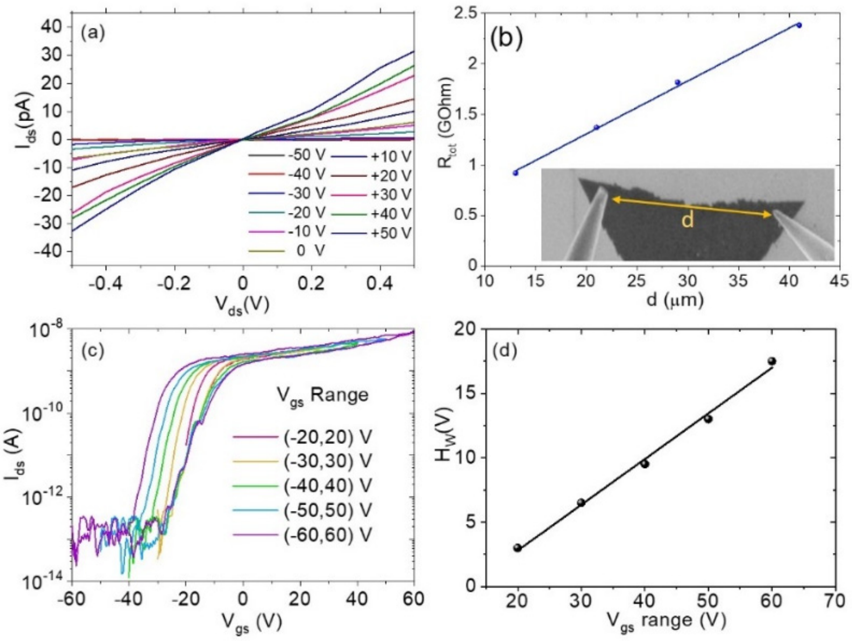

Figure 2. (**a**) Output characteristics ($I_{ds} - V_{ds}$) measured for different gate voltage values. (**b**) R_{tot} vs d plot and linear fit. The inset show how d is measured. (**c**) Transfer characteristics ($I_{ds} - V_{gs}$) measured for different gate voltage ranges. (**d**) Linear dependence of the hysteresis width H_W as a function of V_{gs}.

From the transfer characteristic measured in the range ±50 V, we have estimated the on/off ratio as ~10^5, a subthreshold swing of $SS \approx 4 \frac{V}{decade}$, and a mobility of $\mu = 1\ \text{cm}^2\ \text{V}^{-1}\ \text{s}^{-1}$, a value within the typical range ($0.02 - 100\ \text{cm}^2\ \text{V}^{-1}\ \text{s}^{-1}$) reported for MoS_2-based FETs on SiO_2 [23,24]. The low mobility can be attributed to the high contact resistance and to high defects or traps density [25].

In Figure 3c, we show the transfer characteristics measured by sweeping the gate voltage different ranges, from ±20 V up to ±60 V. The curves have a clear hysteresis that we explain as being caused by negative charge trapping [20]. We observe that the hysteresis width (H_W), estimated at $I_{ds} = 0.1$ nA, has linear dependence on the V_{gs} sweeping range (See Figure 3d). This behavior can be ascribed to the trapping process driven by the gate voltage and the effects on the MoS_2/Si-substrate capacitor.

Finally, we also investigated the field emission (FE) properties of the MoS_2 flake, profiting of the n-type conduction and the high aspect ratio of the flake side. By retracting the tip-anode at a distance h = 900 nm from the MoS_2 edge, we can measure the current emitted from the flake under the application of an external electric field (Figure 3a). More precisely, we applied a voltage bias of up to 120 V on the anode, and we measured the current emitted from the flake (cathode) with a resolution better that 0.1 pA. The current–voltage ($I_{ds} - V_{ds}$) curves have been measured at fixed cathode-anode separation h and for two different values of gate voltage.

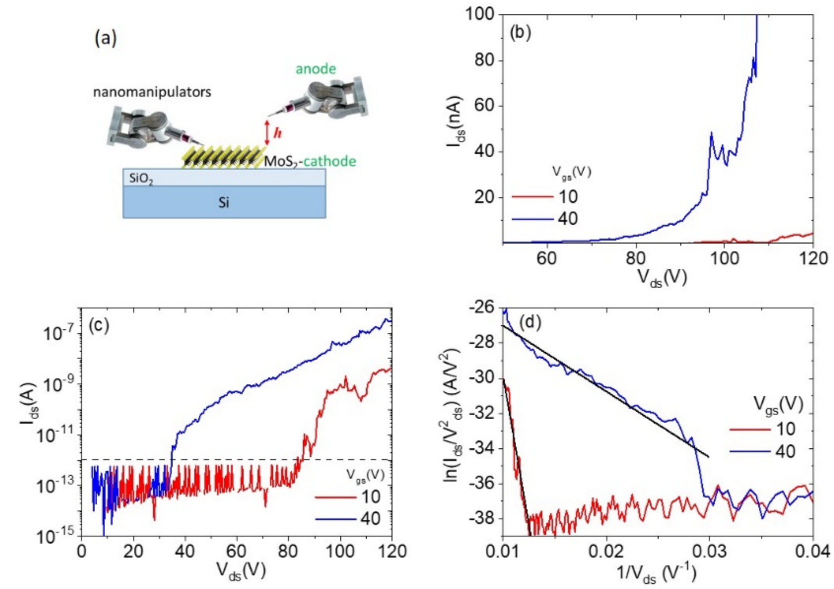

Figure 3. (**a**) Schematic of field emission setup. (**b**) $I_{ds} - V_{ds}$ field emission curves on a linear scale, measured for two different gate voltages. (**c**) Same $I_{ds} - V_{ds}$ field emission curves, reported on a logarithmic scale. (**d**) Fowler-Nordheim plots and linear fittings.

The FE characteristics have been measured by applying a bias voltage on the anode up to +120 V, by keeping a fixed gate voltage of 10 V and 40 V, respectively. The measured curves are reported on a linear scale (Figure 3b) and on a logarithmic scale (Figure 3c). Interestingly, we observe that the FE current is larger for $V_{gs} = 40$ V, suggesting that the gate voltage increases the n-doping of the MoS_2 flake [26].

We analyzed the FE curves in the framework of the Fowler-Nordheim (FN) theory [27], for which the FE current is expressed as

$$I_{ds} = A\frac{(\beta V_{ds}/h)^2}{\Phi} S \cdot exp\left(-B\frac{\Phi^{\frac{3}{2}}}{(\beta V_{ds}/h)}\right),$$

where $A = 1.54 \times 10^{-6}$ A V^{-2} eV and $B = 6.83 \times 10^{7}$ V cm^{-1} eV$^{-3/2}$, Φ is the work function of the emitter, S is the emitting surface area, and β is the field enhancement factor. Accordingly, for FE curves, it is expected that $ln(I_{ds}/V_{ds}^{2})$ versus $1/V$ is linear (FN plot), and β can be evaluated from its slope.

In Figure 3d, we report the FN plots that demonstrate the FE nature of the measured current. For $V_{gs} = 40$ V, we found a turn-on field $E_{on} = 40$ V μm^{-1} (defined as the field to obtain a FE current of 1 pA) and $\beta \approx 200$.

4. Conclusions

We demonstrate a simple and fast methodology to realize metal contacts on two-dimensional nanosheets by gently approaching nanomanipulated tungsten tips inside a scanning electron microscope. We contacted a MoS_2 monolayer to form a back-gated FET, and we performed complete electrical characterization, reporting specific area contact resistivity of 4×10^{-2} Ω cm^2, sheet resistance of 10^8 Ω/□, on/off ratio of 10^5, subthreshold swing of 4 V/decade, and mobility of 1 cm^2 V^{-1} s^{-1}. Finally, by retracting the tip-anode, we performed field emission characterization of the MoS_2 flake, reporting that the FE current can be modulated by the gate bias.

Data Availability Statement: Data available on request.

Conflicts of Interest: The authors declare no conflict of interest.

References

1. Tong, X.; Ashalley, E.; Lin, F.; Li, H.; Wang, Z.M. Advances in MoS2-Based Field Effect Transistors (FETs). *Nano-Micro Lett.* **2015**, *7*, 203–218, doi:10.1007/s40820-015-0034-8.
2. Seo, D.; Lee, D.Y.; Kwon, J.; Lee, J.J.; Taniguchi, T.; Watanabe, K.; Lee, G.-H.; Kim, K.S.; Hone, J.; Kim, Y.D.; et al. High-performance monolayer MoS2 field-effect transistor with large-scale nitrogen-doped graphene electrodes for Ohmic contact. *Appl. Phys. Lett.* **2019**, *115*, 012104, doi:10.1063/1.5094682.
3. Di Bartolomeo, A.; Grillo, A.; Urban, F.; Iemmo, L.; Giubileo, F.; Luongo, G.; Amato, G.; Croin, L.; Sun, L.; Liang, S.-J.; et al. Asymmetric Schottky Contacts in Bilayer MoS_2 Field Effect Transistors. *Adv. Funct. Mater.* **2018**, *28*, 1800657, doi:10.1002/adfm.201800657.
4. Divya Bharathi, N.; Sivasankaran, K. Research progress and challenges of two dimensional MoS2 field effect transistors. *J. Semicond.* **2018**, *39*, 104002, doi:10.1088/1674-4926/39/10/104002.
5. Hao, L.; Liu, Y.; Gao, W.; Han, Z.; Xue, Q.; Zeng, H.; Wu, Z.; Zhu, J.; Zhang, W. Electrical and photovoltaic characteristics of MoS_2/Si *p-n* junctions. *J. Appl. Phys.* **2015**, *117*, 114502, doi:10.1063/1.4915951.
6. Lopez-Sanchez, O.; Lembke, D.; Kayci, M.; Radenovic, A.; Kis, A. Ultrasensitive photodetectors based on monolayer MoS2. *Nat. Nanotechnol.* **2013**, *8*, 497–501, doi:10.1038/nnano.2013.100.
7. Di Bartolomeo, A.; Genovese, L.; Foller, T.; Giubileo, F.; Luongo, G.; Croin, L.; Liang, S.-J.; Ang, L.K.; Schleberger, M. Electrical transport and persistent photoconductivity in monolayer MoS_2 phototransistors. *Nanotechnology* **2017**, *28*, 214002, doi:10.1088/1361-6528/aa6d98.
8. Fu, H.; Yu, K.; Li, H.; Li, J.; Guo, B.; Tan, Y.; Song, C.; Zhu, Z. Enhanced field emission and photocatalytic performance of MoS_2 titania nanoheterojunctions via two synthetic approaches. *Dalton Trans.* **2015**, *44*, 1664–1672, doi:10.1039/C4DT03035D.
9. Kashid, R.V.; Late, D.J.; Chou, S.S.; Huang, Y.-K.; De, M.; Joag, D.S.; More, M.A.; Dravid, V.P. Enhanced Field-Emission Behavior of Layered MoS_2 Sheets. *Small* **2013**, *9*, 2730–2734, doi:10.1002/smll.201300002.
10. Giubileo, F.; Grillo, A.; Passacantando, M.; Urban, F.; Iemmo, L.; Luongo, G.; Pelella, A.; Loveridge, M.; Lozzi, L.; Di Bartolomeo, A. Field Emission Characterization of MoS2 Nanoflowers. *Nanomaterials* **2019**, *9*, 717, doi:10.3390/nano9050717.
11. Giubileo, F.; Iemmo, L.; Passacantando, M.; Urban, F.; Luongo, G.; Sun, L.; Amato, G.; Enrico, E.; Di Bartolomeo, A. Effect of Electron Irradiation on the Transport and Field Emission Properties of Few-Layer MoS_2 Field-Effect Transistors. *J. Phys. Chem. C* **2019**, *123*, 1454–1461, doi:10.1021/acs.jpcc.8b09089.
12. Li, P.; Zhang, D.; Sun, Y.; Chang, H.; Liu, J.; Yin, N. Towards intrinsic MoS_2 devices for high performance arsenite sensing. *Appl. Phys. Lett.* **2016**, *109*, 063110, doi:10.1063/1.4960967.
13. Yan, L.; Shi, H.; Sui, X.; Deng, Z.; Gao, L. MoS_2 -DNA and MoS_2 based sensors. *RSC Adv.* **2017**, *7*, 23573–23582, doi:10.1039/C7RA02649H.
14. Sun, J.; Li, X.; Guo, W.; Zhao, M.; Fan, X.; Dong, Y.; Xu, C.; Deng, J.; Fu, Y. Synthesis Methods of Two-Dimensional MoS2: A Brief Review. *Crystals* **2017**, *7*, 198, doi:10.3390/cryst7070198.
15. Mak, K.F.; Lee, C.; Hone, J.; Shan, J.; Heinz, T.F. Atomically Thin MoS 2: A New Direct-Gap Semiconductor. *Phys. Rev. Lett.* **2010**, *105*, doi:10.1103/PhysRevLett.105.136805.
16. Lee, Y.T.; Kang, J.-H.; Kwak, K.; Ahn, J.; Choi, H.T.; Ju, B.-K.; Shokouh, S.H.; Im, S.; Park, M.-C.; Hwang, D.K. High-Performance 2D MoS2 Phototransistor for Photo Logic Gate and Image Sensor. *ACS Photonics* **2018**, *5*, 4745–4750, doi:10.1021/acsphotonics.8b01049.
17. Giubileo, F.; Di Bartolomeo, A. The role of contact resistance in graphene field-effect devices. *Prog. Surf. Sci.* **2017**, *92*, 143–175, doi:10.1016/j.progsurf.2017.05.002.
18. Giubileo, F.; Di Bartolomeo, A.; Martucciello, N.; Romeo, F.; Iemmo, L.; Romano, P.; Passacantando, M. Contact resistance and channel conductance of graphene field-effect transistors under low-energy electron irradiation. *Nanomaterials* **2016** *6* (*11*), 206, doi: 10.3390/nano6110206.
19. Urban, F.; Lupina, G.; Grillo, A.; Martucciello, N.; Di Bartolomeo, A. Temperature and gate effects on contact resistance and mobility in graphene transistors by TLM and Y-function methods. *arXiv* **2019**, arXiv:1912.04623.
20. Di Bartolomeo, A.; Genovese, L.; Giubileo, F.; Iemmo, L.; Luongo, G.; Foller, T.; Schleberger, M. Hysteresis in the transfer characteristics of MoS_2 transistors. *2D Mater.* **2017**, *5*, 015014, doi:10.1088/2053-1583/aa91a7.
21. Qi, L.; Wang, Y.; Shen, L.; Wu, Y. Chemisorption-induced *n* -doping of MoS_2 by oxygen. *Appl. Phys. Lett.* **2016**, *108*, 063103, doi:10.1063/1.4941551.
22. Cho, K.; Kim, T.-Y.; Park, W.; Park, J.; Kim, D.; Jang, J.; Jeong, H.; Hong, S.; Lee, T. Gate-bias stress-dependent photoconductive characteristics of multi-layer MoS_2 field-effect transistors. *Nanotechnology* **2014**, *25*, 155201, doi:10.1088/0957-4484/25/15/155201.
23. Bao, W.; Cai, X.; Kim, D.; Sridhara, K.; Fuhrer, M.S. High mobility ambipolar MoS_2 field-effect transistors: Substrate and dielectric effects. *Appl. Phys. Lett.* **2013**, *102*, 042104, doi:10.1063/1.4789365.
24. Radisavljevic, B.; Kis, A. Mobility engineering and a metal–insulator transition in monolayer MoS2. *Nat. Mater.* **2013**, *12*, 815–820, doi:10.1038/nmat3687.

25. Urban, F.; Giubileo, F.; Grillo, A.; Iemmo, L.; Luongo, G.; Passacantando, M.; Foller, T.; Madauß, L.; Pollmann, E.; Geller, M.P.; et al. Gas dependent hysteresis in MoS_2 field effect transistors. *2D Mater.* **2019**, *6*, 045049, doi:10.1088/2053-1583/ab4020.
26. Di Bartolomeo, A.; Urban, F.; Passacantando, M.; McEvoy, N.; Peters, L.; Iemmo, L.; Luongo, G.; Romeo, F.; Giubileo, F. A WSe_2 vertical field emission transistor. *Nanoscale* **2019**, *11*, 1538–1548, doi:10.1039/C8NR09068H.
27. Fowler, R.H.; Nordheim, L. Electron Emission in Intense Electric Fields. *Proc. R. Soc. A Math. Phys. Eng. Sci.* **1928**, *119*, 173–181, doi:10.1098/rspa.1928.0091.